Scilight

Photochemistry and Spectroscopy
https://www.sciltp.com/journals/ps

Article

S_2 Emission and Conformational Landscapes: System Specific Excited-State Photophysics in 1,2-Dicarbonyls

Pronab Kundu [1,*], K. N. Venkataravana [1] and Nitin Chattopadhyay [2,3,4,*]

[1] Department of Chemistry, Presidency University, Bengaluru 560119, Karnataka, India
[2] Department of Chemistry, Jadavpur University, Kolkata 700032, West Bengal, India
[3] School of Studies in Chemistry, Pandit Ravishankar Shukla University, Raipur 492010, Chhattisgarh, India
[4] Department of Chemistry, Dr. C. V. Raman University, Kargi Road, Bilaspur 495113, Chhattisgarh, India
* Correspondence: pronabkunduchem@gmail.com (P.K.); nitin.chattopadhyay@yahoo.com (N.C.)

How To Cite: Kundu, P.; Venkataravana, K.N.; Chattopadhyay, N. S_2 Emission and Conformational Landscapes: System Specific Excited-State Photophysics in 1,2-Dicarbonyls. *Photochemistry and Spectroscopy* **2025**, *1*(1), 1.

Received: 16 June 2025
Revised: 19 August 2025
Accepted: 27 August 2025
Published: 29 August 2025

Abstract: Photophysics of 1,2-dicarbonyl compounds—benzil being a classic example—exhibiting multiple emissions has been the subject of extensive investigation over the past decades, targeting principally to their interesting, so called, *cis-trans* photoisomerization. Despite a host of explorations, several issues remained obscured, such as assignment of the high energy fluorescence observed in benzil and α-naphthil, as well as the possible coexistence of multiple conformers in the photoexcited states. The present account, mostly based on a series of our own experiments combining indigenous as well as state-of-the-art steady-state and time-resolved spectroscopic techniques, supported by quantum chemical calculations, offers an in-depth exploration of the complex photophysics of a series of 1,2-dicarbonyl compounds namely, benzil, α-naphthil, 2,2′-pyridil, α-furil, and 9,9′-anthril. The pioneering and ground-breaking features of the report include assignment of the high energy fluorescence of benzil and α-naphthil to originate from the respective S_2 states, a challenge to Kasha's rule; and coexistence of multiple conformers in the lowest excited singlet as well as triplet states. Interestingly, these characteristics are not found to be general behavior of the 1,2-dicarbonyl family but are very much specific to the individual molecular systems, as validated from the potential energy profiles simulated from the DFT and TDDFT based quantum chemical calculations. While unravelling the complex photophysics involving photoisomerization processes of the molecular systems in the series and capturing the intricate excited-state dynamics therein with enhanced clarity, we have cunningly adopted our pioneering experimental technique of freezing the solutions at 77 K independently in the presence and absence of the exciting radiation. Overall, this vivid and progressive account presents a pivotal step forward in understanding the photophysics of 1,2-dicarbonyl compounds.

Keywords: S_2 emission; Kasha's rule; 1,2-dicarbonyls; photophysics; photoisomerization

1. Introduction

Spectroscopy is a fundamental scientific tool that helps in exploring interactions between matter and light, offering critical insights at the molecular level towards composition, structure, and properties. In molecular spectroscopy, fluorescence and phosphorescence are cornerstone phenomena, serving as powerful gadgets for investigating photophysics of a vast range of molecular systems, leading to a profound impact across various domains of chemistry, medical diagnostics, molecular and structural biology, environmental sensing, forensic science and many more [1,2]. Application of fluorescence spectroscopy in studying excited-state processes like

charge transfer (CT), excited-state inter- or intra-molecular proton transfer (ESPT and ESIPT), *cis-trans* photoisomerization etc. has profound implications for understanding the complex dynamics of molecular systems in both solution and solid phases [1–11]. These processes reveal critical insights into energy distribution, molecular geometry, and excited-state reactivity, offering a deeper understanding of molecular behavior under light excitation. Apart from these, fluorescence has enabled researchers to investigate the single-molecule studies of molecular phenomena within cells, uncovering complex biological processes. Despite these advancements, there still remain several areas in the field of fundamental photophysics where unanswered questions persist, one such being the mysterious photophysics of aromatic 1,2-dicarbonyl compounds.

Regardless of decades of research, complete understanding of the excited-state dynamics, including fluorescence and phosphorescence behavior of 1,2-dicarbonyl compounds, remains incomplete. Among various 1,2-dicarbonyl compounds, benzil has garnered significant attention due to its intriguing photophysical properties and its pioneering role as a model system for studying "*cis-trans*" photoisomerization [12–20]. Early investigations with benzil focused on its absorption, emission, and excitation spectra at low temperatures, providing initial evidence for the occurrence of this phenomenon [14]. Subsequently, theoretical and experimental studies revealed that the molecule undergoes significant geometric changes upon excitation, transitioning from a *skew* ground state configuration to a more planar structure in its excited singlet and/or triplet states [15–17]. Notably, benzil exhibits highly efficient intersystem crossing from the singlet to the triplet manifold, as evidenced by its substantial triplet quantum yield, further reinforcing its role as a model system for studying triplet-state dynamics [18,19].

Despite the wealth of knowledge accumulated on the photoisomerization process of benzil, certain aspects of its fluorescence attribute have remained elusive. Notably, a high-energy fluorescence band observed in solution has been reported but not assigned [21], leaving its origin unclear. This unresolved question inspired us to investigate the unexplored emission of benzil, resulting in our pioneering proposition that the high-energy fluorescence corresponds to emission from the S_2 state [22]. This observation is novel for any 1,2-dicarbonyl system and hence groundbreaking, as fluorescence from higher excited singlet state/s is rare and directly challenges Kasha's rule, which posits that fluorescence typically occurs from the lowest excited singlet (S_1) state [1,2,23]. Our discovery of S_2 emission in benzil not only advances the understanding of photophysics and excited-state dynamics in molecular systems but also extends the list of systems such as azulene, Zn-tetrabenzoporphyrin, thione, 3-hydroxyflavone, BODIPY and carbazole derivatives [24–29], that defy Kasha's rule [Scheme 1].

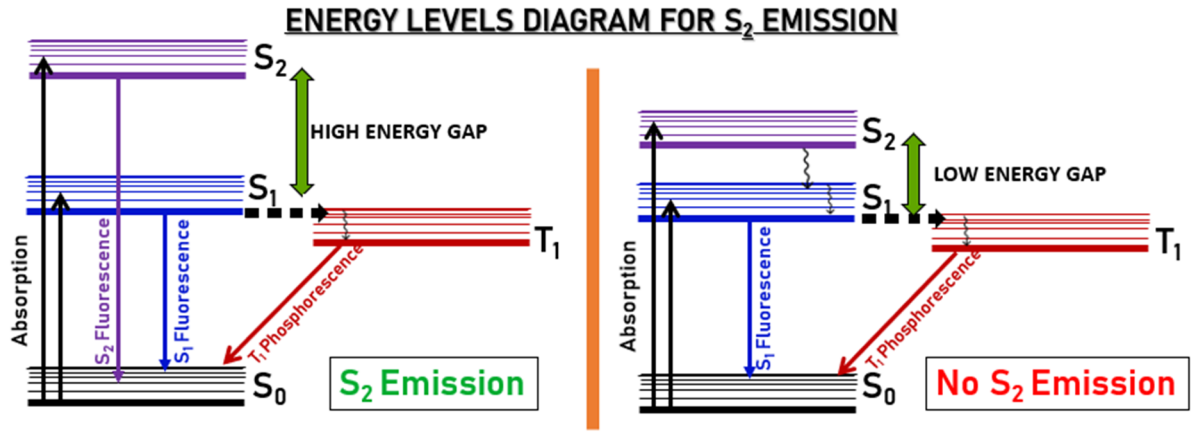

Scheme 1. Energy level diagrams depicting conditions for the observation and non-observation of S_2 emission.

To further explore the phenomenon of S_2 emission and uncover its underlying mechanism, we developed an innovative experimental approach to study the photoisomerization of benzil. This method, pioneered by Chattopadhyay and co-workers, involves freezing the sample solution at 77 K under two distinct conditions—with and without exposure to excitation light [30]. The philosophy is straightforward: if frozen in the absence of the radiation, solid benzil maintains its ground-state geometry, and no fluorescence from the relaxed excited state is feasible in the frozen matrix. However, under excitation radiation in the solution phase, a steady-state dynamic equilibrium is established between the ground-state and excited-state relaxed geometries (conformers). Freezing the solution under such a situation captures this equilibrium state within the rigid matrix, enabling observation of emissions from both the geometric conformers. This novel and unique technique provided unambiguous evidences to unearth photoisomerization in benzil and laid the groundwork for studying other 1,2-dicarbonyl compounds as well [30].

Encouraged by the findings with benzil, we extended our investigations to include other members of the 1,2-dicarbonyl family like α-naphthil, α-furil, 2,2′-pyridil and 9,9′-anthril, to assess whether or not S_2 emission is a general phenomenon for this class of compounds [31–34]. Interestingly, while benzil and α-naphthil exhibited S_2 emission, similar features were absent for the remaining compounds within the family. This indicates that occurrence of S_2 emission is not a generic phenomenon across the 1,2-dicarbonyl series; rather, its occurrence appears to be molecule-specific, governed by the specific energy differences between the photoexcited states as is perceptible from the potential energy curves (PECs) of the individual compounds. These PECs, derived from DFT/TDDFT-based quantum chemical simulations, provided critical theoretical insights into the excited-state behavior supporting the experimental findings.

In addition to the observation of S_2 emission, our investigations uncovered multiple fluorescence and phosphorescence emissions from the 1,2-dicarbonyl compounds under various experimental conditions in fluid (RT) and frozen matrices (77 K). These observations were further analyzed using time-resolved emission spectroscopy (TRES) and time-resolved area normalized emission spectroscopy (TRANES), two techniques that have proven instrumental in resolving overlapping emissions from different excited species. Combination of these time-resolved techniques with the PECs generated from quantum chemical calculations allowed us to assign the multiple emissions to different singlet and triplet state geometries, providing a deeper understanding of the excited-state processes of the studied compounds in the series [22,31–34].

The unorthodox findings reported in this account, including the observation of S_2 emission and exploration of photoisomerization dynamics in 1,2-dicarbonyl compounds, represent significant advancements in the field of photophysics. These discoveries have not only broadened our understanding of the excited-state behavior of benzil and its analogs, but also highlighted the importance of time-resolved techniques and computational methods in unravelling the complexities of molecular photophysics.

In this account, we systematically investigate and report the photophysics of 1,2-dicarbonyl compounds, namely benzil, α-napthil, α-furil, 2,2′-pyridil and 9,9′-anthril [Scheme 2], focusing mostly on the unexplored attributes of their photophysical behavior, including the occurrence of higher energy emissions and the photoisomerization processes in solution and solid phases exploiting experimental and computational analyses. The studies aim to provide a comprehensive understanding of the fundamental photophysical mechanisms governing these molecular systems, with an emphasis on novel observations and theoretical justifications. We believe that this research account will inspire further research in photophysics/photochemistry, and provide a comprehensive framework for investigating the intricate dynamics in new molecular systems.

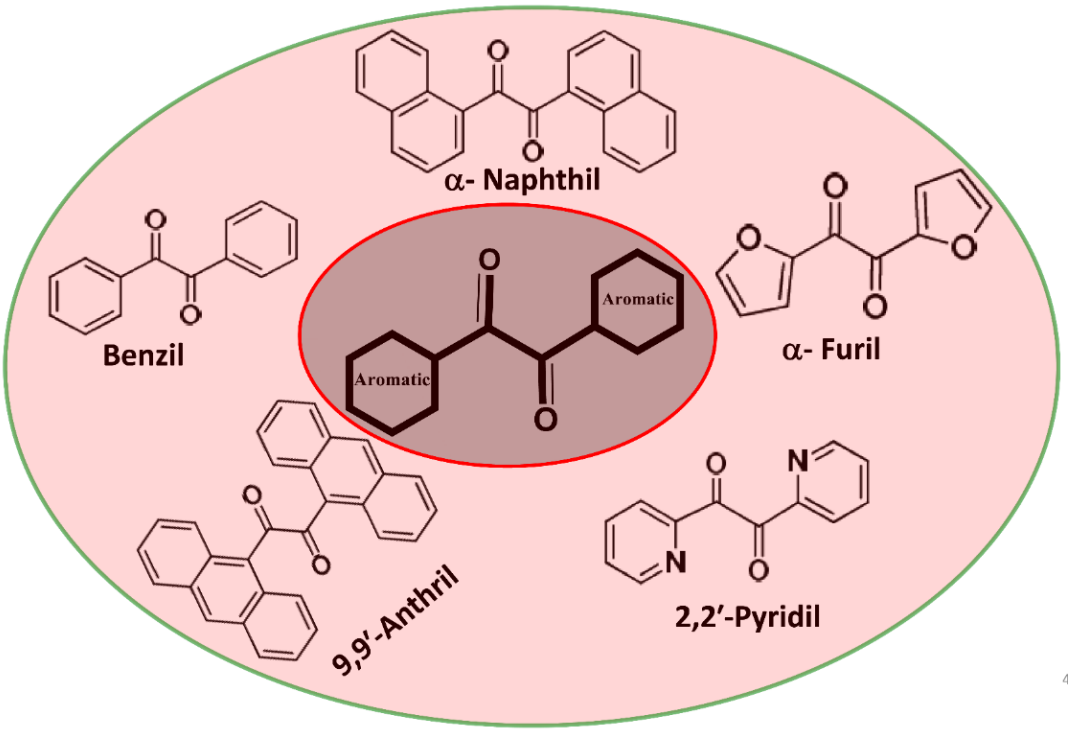

Scheme 2. Chemical structures of the 1,2-dicarbonyl compounds undertaken, namely benzil, α-napthil, α-furil, 2,2′-pyridil and 9,9′-anthril.

2. Benzil System: Beyond Conventional Emissions

Benzil, a prototype of aromatic α-dicarbonyl compounds, has long been studied for its intriguing photophysical/photochemical properties, particularly its conformational flexibility and photoisomerization behavior. Early investigations focused on its low-temperature absorption and emission features, with Bera et al. providing a comprehensive spectral analysis encompassing absorption, emission, and excitation spectra at cryogenic conditions [14]. One of the key photophysical traits of benzil is its capacity to undergo "*cis*-*trans*" photoisomerization from a skewed geometry in the ground state to a *trans*-planar (TP) conformation in the excited state, as evidenced by both crystallographic data and theoretical calculations [15–17]. Arnett and McGlynn offered pivotal insights into its photorotamerism, a process that has been confirmed by multiple spectroscopic and computational studies [35–41]. Quantum chemical calculations by Chan et al. highlighted torsional relaxation in the lowest triplet state [36], while Ray et al. and Bhattacharyya et al. confirmed the geometrical transformation from *skew* to TP configuration using time-resolved spectroscopy and solvent-dependent emission analyses [37,39]. Chattopadhyay et al. further validated this excited-state isomerization using laser-induced optoacoustic spectroscopy, quantifying the intrinsic molar volume changes corresponding to the photo-process [40]. Dynamics of conformational relaxation have also been probed with ultrafast transient absorption spectroscopy [42]. Chattopadhyay et al. even extended the study to supercritical carbon dioxide environment [43].

The inter-carbonyl torsion angle (O=C–C=O), a critical structural parameter governing benzil's spectral properties, has been characterized using X-ray diffraction and DFT calculations, with reported ground-state values near 72° [15,39,44,45]. Benzil's efficient intersystem crossing has made it a model molecule for triplet state studies, including phosphorescence from both *skew* and *trans*-planar conformers under various matrix conditions [37,44]. Surprisingly, despite decades of research, its fluorescence behavior remains poorly characterized even in solution phase [21,39]. Although multiple emission bands have been reported, their exact assignments, particularly for the high-energy band, remain elusive.

At this backdrop, we have undertaken a detailed investigation of benzil's multiple emission bands in both fluid solution and frozen matrix (77 K) environments. Using the novel freezing-illumination protocol developed by our group [30], in combination with time-resolved fluorescence decay analysis, we provide the first conclusive evidence that the high-energy emission of benzil originates from the S_2 state—a rare observation that challenges Kasha's rule. To support the experimental findings, we performed ab initio quantum chemical calculations to generate PECs for various electronic states, thereby offering a theoretical framework to rationalize the S_2 fluorescence and conformational photophysics of benzil.

The room-temperature absorption spectra of benzil recorded in ethanol (EtOH) and methylcyclohexane (MCH) (Figure 1A) confirm a prominent π→π* transition band below 350 nm, along with a weaker, broad n→π* absorption in the 360–440 nm range, as validated by its low intensity and slight hypsochromic shift in polar EtOH. The spectral resemblance to benzaldehyde implies negligible interaction between benzoyl units, consistent with a *skew* geometry in the ground state [39].

When excited at 370 nm (n→π* band) in solution at room temperature, benzil displays dual emission bands (Figure 1B): a band at ~430 (EtOH)/~415 nm (MCH), along with a second band near ~505 nm; attributed to the S_1-state emissions originating from the relaxed *skew* and *trans*-planar (TP) conformers, respectively. The insensitivity of the 505 nm band to solvent polarity and the solvent dependence of the 415/430 nm band supports these assignments. However, upon π→π* excitation (Figure 1C), in addition to the 505 nm band, a strong and structured emission appears at ~360 nm, overwhelming the 415/430 nm emission. This ~360 nm emission is notably blue-shifted relative to the $S_0 \rightarrow S_1$ absorption, indicating that it originates from a direct $S_2 \rightarrow S_0$ transition. The intensity variation with excitation wavelength and the mirror-image resemblance between the emission and excitation spectra strongly indicate its π→π* character. Based on all these, our group, for the first time, designated this emission as S_2 fluorescence—an unambiguous deviation from Kasha's rule and a novel contribution to the literature of photophysics of 1,2-dicarbonyl systems [22]. Possibility of molecular aggregation has been conclusively ruled out, as the absorption–concentration profile strictly follows Beer's law. Fluorescence quantum yields of the S_1 (*skew*: 0.0036; TP: 0.0013) and S_2 (0.012) emissions confirm that while internal conversion ($S_2 \rightarrow S_1 \rightarrow S_0$) persists, direct S_2 emission is significant under π→π* excitation [22].

Emission analyses of benzil in rigid EtOH and MCH glass matrices at 77 K reveal distinct photophysical behavior depending on the freezing conditions. When the matrices were frozen in dark (Figure 1D), a structured, high-energy emission band around 360 nm is observed, attributed to S_2 fluorescence originating from a skewed geometry resembling the one in the ground state. In contrast, the lower-energy emission near 523 nm corresponds to T_1 phosphorescence, as validated by delayed emission measurements (Figure 1E) [37–40]. Remarkably, when samples were frozen under continuous excitation (Figure 1D), the innovative experimental strategy introduced by

our group [30], an additional broad emission emerges at approximately 420 nm, which is attributed to S_1 fluorescence from the relaxed *skew* conformer produced in the excited state. Simultaneous observation of all the three emissions (S_2, S_1, and T_1) under these conditions underscores the critical role of freezing-led conformational locking in distinguishing geometry-specific excited-state emissions. Furthermore, the excitation spectra for S_2 fluorescence at both RT and 77 K exhibit mirror-image symmetry with the corresponding emission spectra (Figure 1F) and deviate from the lowest energy n→π* absorption band, affirming their S_2 (π→π*) origin and thereby establishing the unique, geometry-sensitive nature of S_2 emission in benzil [22].

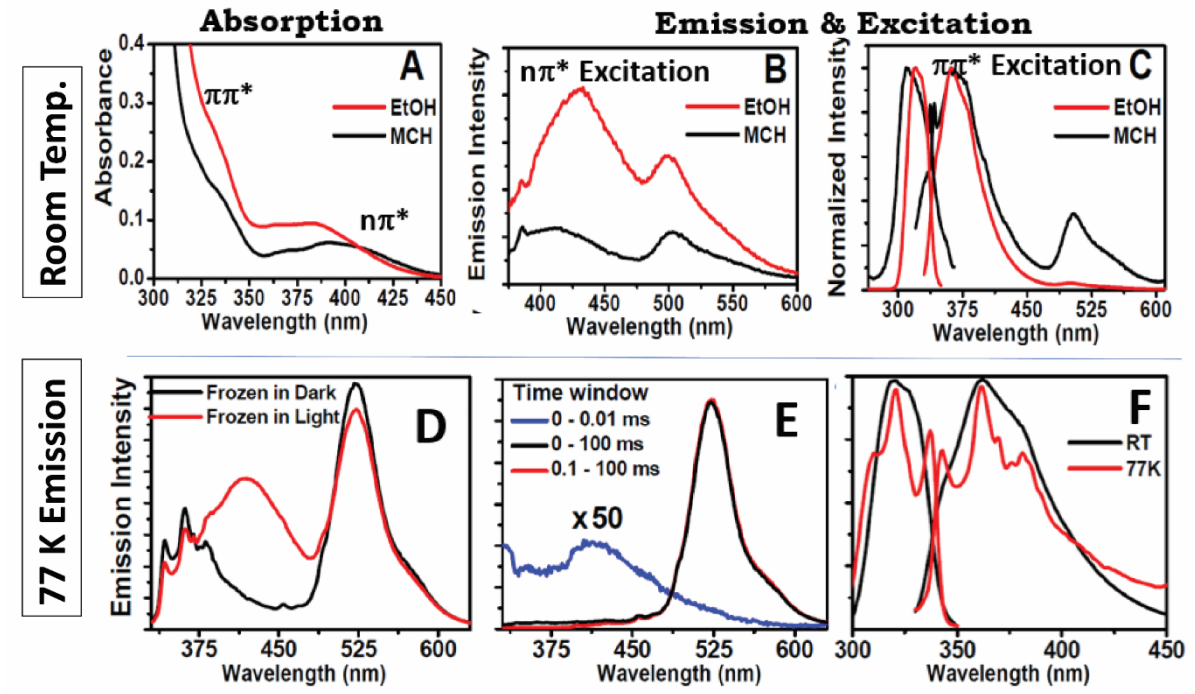

Figure 1. (**A**) Absorption spectra of benzil recorded at room temperature in EtOH and MCH. (**B**) Dual fluorescence observed at RT (λ_{exc} = 370 nm), arising from *skew* and *trans*-planar (TP) conformers. (**C**) Emission (λ_{exc} = 320 nm) and excitation (λ_{em} = 370 nm) spectra revealing strong S_2 fluorescence. (**D**) 77 K emission spectra of benzil in EtOH frozen without (black) and with (red) continuous photoexcitation (λ_{exc} = 320 nm). (**E**) Time-resolved 77 K emission spectra at varying delay times and time windows (λ_{exc} = 320 nm); details in legend. (**F**) Overlay of emission (λ_{exc} = 320 nm) and excitation spectra (λ_{em} = 370 nm) at RT and 77 K, highlighting S_2 fluorescence across conditions. © 2011 AIP Publishing [22].

Time-resolved fluorescence studies of benzil at RT in both EtOH and MCH using excitation wavelengths of 295 nm and 370 nm reveal distinct lifetimes for emissions from different excited-state conformers (Figure 2A,B) [22]. Selective excitation at 295 nm predominantly populates the S_2 state, resulting in monoexponential decay kinetics at 380 nm with a lifetime of approximately 1.3 ns in both solvents. This relatively long-lived S_2 fluorescence is consistent with previously reported fluorophores [46]. The experimental S_2 lifetime was further corroborated by theoretical calculation using the Strickler–Berg equation, which yielded a radiative lifetime of ~1.44 ns [47]. Consistency between the calculated result and experimental data validates the accuracy and dependability of the time-resolved measurements. The emission originating from the S_1 state of the TP conformer (505 nm) exhibits a single-exponential decay (~2.2 ns) that remains unchanged across different solvents and excitation wavelengths, indicating a well-defined and stable *trans*-planer excited-state geometry. In contrast, 420 nm emission, attributed to the *skew* geometry in the S_1 state, demonstrates biexponential decay with dominant short-lived component (~92%, ~200 ps) corresponding to the relaxed-*skew* conformer, while a minor long-lived contribution (~8%, ~2.2 ns) likely arises from partial spectral overlap with the *trans* planar S_1 (TP-S_1) emission [22]. These distinct lifetime components robustly confirm involvement of at least three emissive species in benzil, each associated with specific electronic states and conformational geometries. Moreover, similarity of the decay parameters across both polar and nonpolar solvents suggests that the excited-state dynamics of benzil are predominantly governed by intrinsic molecular properties rather than solvent interactions.

To substantiate experimental assignments of the multiple emission features observed for benzil, ab initio DFT-based potential energy curves (PECs) were simulated for torsional rotation around the O=C–C=O (Φ) in the

S_0 and excited singlet states (S_1, S_2, and S_3) (Figure 2C). For each fixed Φ, all other structural parameters were optimized. The S_0 minimum corresponds to a *skew* conformation (Φ = 126.64°), in agreement with literature reports [22,44.45]. In the S_1 state, a barrierless path connects the Franck–Condon (FC) geometry to a relaxed *trans*-planar (TP) form while an alternate *skew*-like conformation, closer to a *cis* structure, may also be accessed depending on the amount of excitation energy. This suggests dual fluorescence: ~450 nm from the relaxed *skew* form and ~513 nm from the TP geometry, aligning with experimental bands at ~415–430 nm and ~505 nm, respectively. The S_2 state retains a geometry similar to S_0, with an emission calculated at ~375 nm, consistent with the observed ~360 nm band. The large energy difference of 37.16 kJ/mol between the relaxed S_2 and S_1 states supports the possibility of observable $S_2 \rightarrow S_0$ fluorescence, as noted in earlier reports [38,39].

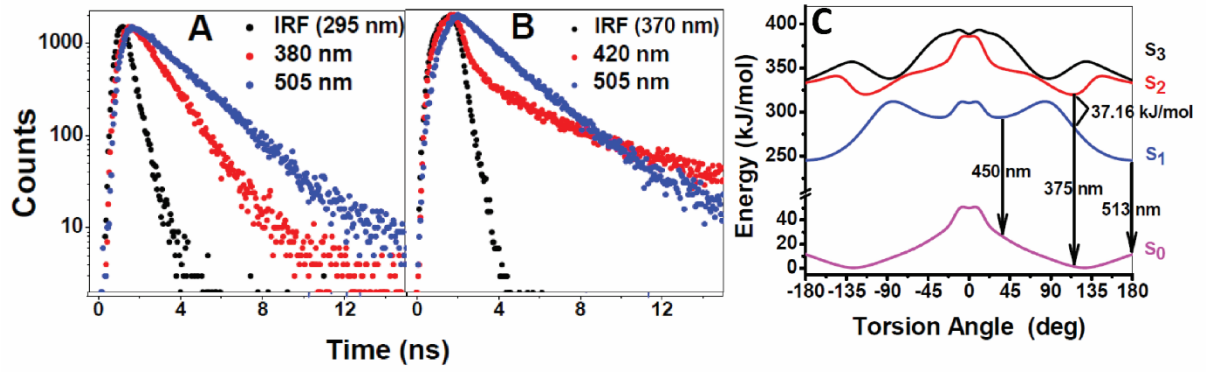

Figure 2. Fluorescence lifetime decay curves of benzil in ethanol recorded at various emission wavelengths (as indicated in the legends) upon excitation at 295 nm (**A**) and 370 nm (**B**). (**C**) S_0, S_1, S_2, and S_3 PECs of benzil plotted against the torsional angle around the O=C–C=O moiety (Φ). © 2011 AIP publications [22].

Taken together, the DFT/TDDFT-based results provide strong theoretical support for the interpretation of benzil's multi-band fluorescence, including the conclusive observation of S_2-state emission, an explicit violation of Kasha's rule. While emission from the S_1 state originates from both relaxed *skew* and *trans*-planar conformations, S_2 emission arises exclusively from the *skew* geometry. These insights into the excited-state dynamics of α-dicarbonyl systems not only deepen our understanding of photophysics of benzil but also motivate us for further investigations of structurally related molecular systems within the 1,2-dicarbonyl family, namely α-naphthil, 2,2′-pyridil, α-furil, and 9,9′-anthril.

3. Extension to α-Naphthil: Evidence of S_2-State Fluorescence beyond Benzil

Exploring as a pioneer and assigning the S_2 fluorescence in benzil, a finding that challenges the conventional Kasha-compliant emission paradigms, we extended our investigation to α-naphthil, a structural analog within the same 1,2-dicarbonyl family [31]. Although the spectral and phosphorescence properties of α- and β-naphthil have been explored extensively in diverse environments such as fluid solutions, frozen matrices, and molten glassy states, majority of the earlier studies predominantly concentrated on their phosphorescence emissions and photoisomerization dynamics [37,48–51]. Notably, Herkstroeter et al. reported dual phosphorescence from β-naphthil, attributed to the existence of *cisoid* and *transoid* conformers in the triplet excited state [48]. Additional evidence from flash photolysis and time-resolved spectroscopy confirmed the presence of these conformers, and highlighted the role of geometrical relaxation processes within the triplet state [37,50].

Despite these advances, the prospect of S_2-state fluorescence in α-naphthil had remained largely unexplored. Self-inspired by our discovery of S_2 emission in benzil [22], we undertook a systematic and comprehensive investigation to probe the possibility of a similar radiative deactivation pathway from higher excited singlet states in α-naphthil [31]. Employing an integrated experimental approach—combining steady-state and time-resolved fluorescence spectroscopy at room temperature and 77 K together with supporting quantum chemical calculations of potential energy curves, this study presented the first definitive evidence of S_2 fluorescence from α-naphthil. The combined spectroscopic and computational results not only confirmed the presence of emission from higher excited singlet-state but also provided robust theoretical justification for the observed photophysical phenomenon. The findings significantly enrich our understanding of the excited-state dynamics in aromatic 1,2-dicarbonyl systems, revealing the broader potential of S_2-state fluorescence in such flexible molecular frameworks. This discovery opens new avenues for re-evaluating excited-state dynamics in similar molecular systems, questioning the universality of the traditional Kasha's rule.

Absorption studies of α-naphthil at RT in both EtOH and MCH solvents reveal distinct n→π* (400–450 nm, weak) and π→π* transitions (280–370 nm, strong) (Figure 3A), with solvent-dependent spectral shifts confirming the nature of these electronic transitions. Similarity of the n→π* band to that of α-naphthaldehyde, along with IR evidence (split C=O band), supports a puckered C_2-symmetric *skew* conformation for α-naphthil in the ground state [31,52,53].

Photoexcitation of α-naphthil at its n→π* band (425 nm), structured fluorescence is observed near 490 nm in both polar and nonpolar solvents (Figure 3B). The lack of a complete mirror-image relationship between the excitation and emission spectra suggests that significant geometric relaxation occurs in the S_1 state. Interestingly, excitation at the higher-energy π→π* band (340 nm) dramatically alters the emission profile, producing an intense and unstructured fluorescence peaking at ~423 nm (Figure 3C), not reported in the existing literature. This high-energy emission, appearing above the onset of $S_0 \rightarrow S_1$ absorption energy, is unambiguously attributable to $S_2 \rightarrow S_0$ fluorescence, consistent with earlier findings with benzil [22]. The prominent intensity and higher energy of this emission further reinforce its π→π* origin, distinguishing it from the weaker S_1 fluorescence of n→π* character. Concentration-dependent absorption measurements show no spectral shifts or new features, confirming the monomeric nature of the species and rules out aggregation-related effects [31].

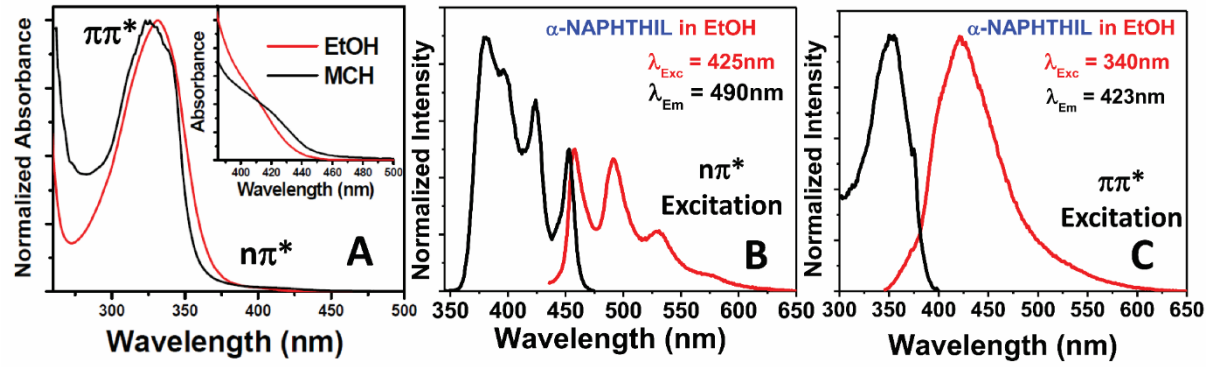

Figure 3. (**A**) Absorption spectra of α-naphthil in EtOH and MCH at RT. Emission (red) and excitation (black) spectra corresponding to (**B**) nπ* excitation (λ_{exc} = 425 nm) and (**C**) ππ* excitation (λ_{exc} = 340 nm) of α-naphthil in EtOH. © 2012 ACS publication [31].

Low-temperature (77 K) emission analyses of α-naphthil in rigid ethanol matrices reveal multiple structured emissions originating from distinct excited states and conformations. Excitation at the n→π* (425 nm) and π→π* (340 nm) bands revealed three distinct emissions: (i) a structured fluorescence centered around 460 nm ($S_1 \rightarrow S_0$), (ii) a lower-energy structured emission band near 520 nm, and (iii) a higher-energy $S_2 \rightarrow S_0$ fluorescence at ~423 nm, specifically upon excitation at the 340 nm band (Figure 4A). These emissions arise from molecular conformers frozen in geometries close to those in the ground state, since the rigid matrix inhibits torsional relaxation. Delayed time window (0.1–1000 ms) emission and time-resolved measurements confirmed the phosphorescence characteristics of the 510–625 nm emission, with a decay time of 126 ± 10 ms independent of monitoring wavelength, indicating origin of the emission from a triplet state. In contrast, emissions observed at ~423 nm and ~460 nm were confirmed as fluorescence due to their detection within a short time window (0–0.02 ms), clearly separating them from the long-lived phosphorescence signals (Figure 4B).

When the ethanolic solution of α-naphthil was frozen under continuous illumination at 340 nm, a new and weak emission emerged at ~524 nm. This emission was absent when the solution was frozen under dark. This emission is, therefore, attributed to the relaxed *trans* conformer that was formed in the photoexcited state in solution phase under equilibrium which was subsequently frozen to solid matrix. This 524 nm emission was extracted by subtracting the fluorescence spectrum collected in the matrix frozen under dark from the same of the matrix frozen under continuous light excitation (Figure 4C). Our illumination-freezing strategy uniquely reveals fluorescence from the photogenerated *trans* conformer, which is otherwise masked under room-temperature solution phases or dark-frozen 77 K matrices.

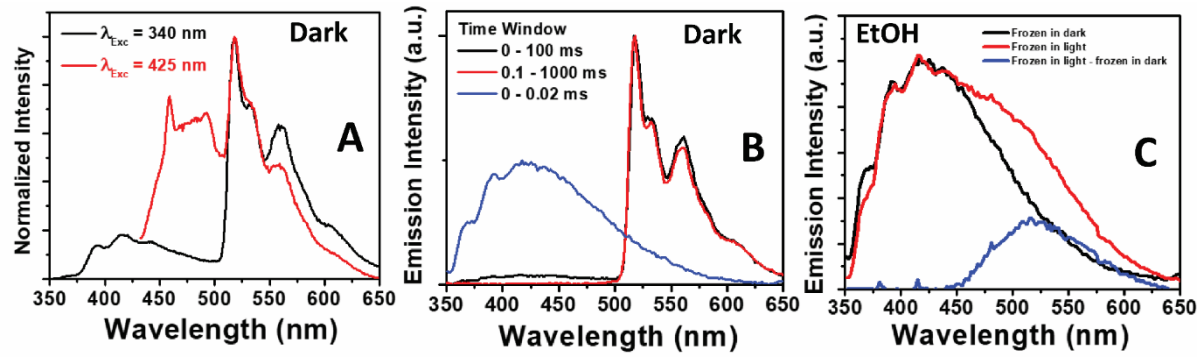

Figure 4. (**A**) Emission spectra of α-naphthil recorded in EtOH matrix at 77 K, frozen without light exposure, under different excitation wavelengths as specified. (**B**) Time-resolved fluorescence and phosphorescence spectra were acquired upon excitation at 340 nm across selected time windows. (**C**) Fluorescence spectrum corresponding to the *trans* conformer was isolated by subtracting spectra of samples frozen under 340 nm irradiation (red) and in the dark (black), both captured within the 0–0.02 ms time window to eliminate phosphorescence contributions. The resulting difference spectrum is shown in blue. © 2012 ACS publication [31].

Time-resolved fluorescence decay measurements of α-naphthil in ethanol at RT, with excitations at 450 nm (n→π*) and 370 nm (π→π*), reveal three distinct emissive species corresponding to different electronic states and molecular conformations (Figure 5A). Excitation at 450 nm yielded bi-exponential decays at 490 and 530 nm with lifetimes of 1.3 ± 0.3 ns and 4.0 ± 0.4 ns, where the dominant shorter-lived component corresponds to the relaxed *skew* conformer in the S_1 state, and the longer-lived minor component is attributed to the weakly emissive *trans* conformer. Under 370 nm excitation, tri-exponential decays were observed with lifetimes 0.73 ± 0.1 ns, 1.3 ± 0.3 ns, and 4.0 ± 0.4 ns [31]. The shortest lifetime component, dominant across the emission window 420–550 nm range, is attributed to S_2 fluorescence originating from the skewed conformer retaining a geometry close to that in the ground state. Its absence under lower energy nπ* excitation approves this assignment. The intermediate and long-lived components represent S_1 emissions from the relaxed *skew* and *trans* forms, respectively. The increasing contribution of the longer-lived components toward the red edge of the spectrum further supports this interpretation. These results establish the coexistence of three emissive species: $S_2 \rightarrow S_0$ emission (0.73 ns) from the ground-state like geometry, $S_1 \rightarrow S_0$ emission (1.3 ns) from the relaxed *skew* form, and $S_1 \rightarrow S_0$ emission (4.0 ns) from the *trans* conformer, underscoring the complex excited-state dynamics of α-naphthil and the role of conformational flexibility in its multi-channel emission behavior.

Ab initio DFT and TDDFT based potential energy curve (PEC) analysis of α-naphthil against the torsional angle around the O=C–C=O moiety provides persuasive theoretical support for the experimentally observed multiple emissions (Figure 5B) [31]. The ground-state PEC reveals a global minimum at a *skew* conformation, confirming the non-planar geometry, as inferred from IR studies. In the S_1 state, the molecule can undergo barrierless relaxation from the Franck–Condon region to either a *trans* or an alternate *skew*-like geometry closer to a *cisoid* form, depending on the excitation energy, rationalizing the dual S_1 emissions—originating from relaxed *trans* and *skew* conformers (Figure 5B). Furthermore, the S_2-state PEC indicating a little deviation from the ground-state geometry, coupled with a significant S_2–S_1 energy gap (~19 kJ/mol), provides a theoretical justification for the observed S_2 emission, mirroring similar behavior reported for benzil. These quantum chemical calculations, thus, offer a robust framework for rationalizing the experimental assignments of S_1 and S_2 fluorescences in α-naphthil.

Therefore, the detailed photophysical studies on α-naphthil have provided evidence of multiple emission pathways, notably identifying a distinct fluorescence band around 423 nm originating from S_2 state, attributed to a conformer retaining near ground-state geometry [31]. Comprehensive investigations combining steady-state and time-resolved fluorescence analyses at both ambient and cryogenic temperatures, complemented by quantum chemical calculations, demonstrate that this geometry is capable of dual emission from both the S_2 and S_1 states, contingent on the excitation wavelength, while an additional emission originates from the photo-produced *trans* conformer. Detection of the respective S_2 fluorescences from both benzil and α-naphthil prompts a pivotal question: is S_2 emission a general photophysical phenomenon for the 1,2-dicarbonyl compounds, or is it restricted to specific molecular frameworks? This burning question stimulated us for further systematic investigations across this class of molecules.

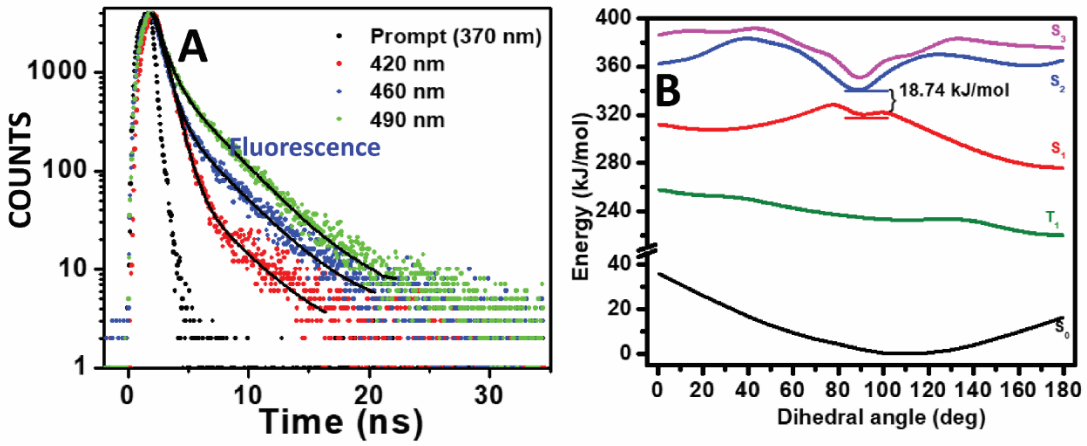

Figure 5. (**A**) Time resolved fluorescence decay profiles of α-naphthil in EtOH at RT; under different monitoring wavelengths as specified. (**B**) Potential energy curves of α-naphthil in various electronic states against the O=C─C=O torsion angle (Φ), illustrating the conformational dependence of excited-state energetics. © 2012 ACS publication [31].

4. 2,2′-Pyridil: Absence of S_2 Emission Despite Structural Analogy with Benzil and α-Naphthil

Following the remarkable identification of S_2 fluorescence from two canonical 1,2-dicarbonyl systems—benzil [22] and α-naphthil [31], we were tempted to extend our photophysical investigations to 2,2′-pyridil, aiming to probe whether this analogue shares a similar excited-state behavior or diverges fundamentally.

Single-crystal X-ray diffraction study reveals that 2,2′-pyridil adopts a *skew* conformation in the ground state, with C_2 symmetry, a dihedral twist of ~83° between the pyridine-carbonyl planes, and an inter-carbonyl angle of ~96.5° [53–56]. Hydrogen bonding in polar solvents further induces conformational flexibility through rotation about the central C–C bond [57]. Earlier studies by Sarkar and Chakravorti [58] reported dual fluorescence in EtOH, ascribed to two rotameric species (*skew* and *trans*), whereas in non-polar solvents, only the *skew*-associated emission persists. Revisiting and expanding upon this, we undertook a focused investigation into the potential of S_2 emission. Through selective photoexcitation and time-resolved spectroscopy at both ambient and 77 K in EtOH and MCH, fluorescence and phosphorescence channels were clearly deconvoluted, as previously accomplished for benzil and α-naphthil. Strikingly, no S_2 emission was observed for 2,2′-pyridil, in direct contrast to its structural congeners. To rationalize this behavior, DFT and TDDFT calculations were employed, revealing a minimal energy separation between the S_2 and S_1 states. This near-degeneracy in energy promotes efficient internal conversion from S_2 to S_1, effectively suppressing any observable S_2 fluorescence.

At room temperature, dilute solutions of 2,2′-pyridil in EtOH and MCH exhibit two strong absorption bands centred around 235 nm and 270 nm (Figure 6A), with negligible solvent shift—indicative of π→π* transitions, consistent with 2-acetylpyridine analogues [59]. At higher concentrations, weaker low-energy bands emerge in 320–420 nm range in both solvents, attributed to n→π* transitions [33,56–58]. These bands likely arise from overlapping $n_{(N)}$→π* and $n_{(O)}$→π* transitions, leading to broadening and obscuring solvent-dependent shifts. Notably, a broad and weak absorption peak at ~435 nm was observed in EtOH, assigned to a singlet-to-triplet (S_0→T_1) transition based on its resemblance with the phosphorescence excitation spectrum [58,60]. Although heavy atoms usually enhance such transitions, absence of any noticeable increase in emission upon addition of KI or KBr suggests a geometry-forbidden transition due to the non-planar alignment between the ground (S_0) and triplet (T_1) states [58,60,61].

Upon n→π* excitation, 2,2′-pyridil exhibits a structured fluorescence band in EtOH (400–650 nm) and MCH (390–550 nm) (Figure 6B). Identical excitation spectra across emission wavelengths confirm a common, non-aggregated emissive species. While Sarkar and Chakravorti have attributed this emission to a *trans*-planar conformational form [58], the TDDFT results indicate a near-*trans* S_1 geometry (dihedral ~170°) (Figure 6I) [33]. The red-shifted emission in EtOH relative to MCH further supports a non-planar, dipolar structure—unlike the planar *trans* forms of benzil and α-furil [22,32]. Excitation into the π→π* band leads to new emissions: ~400 nm in EtOH and ~340 nm in MCH (Figure 6C). These spectral shifts, along with mismatch between absorption and excitation profiles, indicate excited-state conformational transformation. Although initially suggestive of S_2 emission (as seen in benzil and α-naphthil), this assignment was invalidated by the longer lifetime (5.5 ± 0.5 ns) of the higher-energy emission compared to the lower-energy band (1.1 ± 0.1 ns). Instead, TDDFT calculations reveal near-degeneracy between the S_2 minimum and the S_1 crest ($\Delta E \approx 1$ kJ/mol), promoting ultrafast internal

conversion and, thus, negating the possibility of S_2 fluorescence. Instead, the high-energy band originates from a relaxed *skew* S_1 conformer (dihedral ~30°), corroborated by TRANES analysis, which confirm both the emission bands to originate from distinct S_1-state conformers (Figure 6G–I) [33].

Time-resolved fluorescence studies of 2,2′-pyridil upon 370 nm (n→π*) and 300 nm (π→π*) excitations reveal that dual emission arises from two distinct S_1-state conformers—near-*trans* and relaxed *skew*—whose populations were dependent on excitation-wavelength as well as solvent (Figure 6E,F). Bi-exponential decay kinetics in EtOH and MCH upon π→π* excitation, along with lifetime-resolved assignments, confirm that direct excitation to S_2 leads to ultrafast internal conversion followed by relaxation to multiple S_1 conformers. The mono-exponential decay with lifetime 1.1 ± 0.1 ns in MCH under n→π* excitation confirms exclusive emission from the near-*trans* conformer, while bi-exponential decays in both solvents yield lifetimes of 1.69 ± 0.2 ns (*skew*) and 6.8 ± 0.5 ns (near-*trans*) in ethanol, and 5.5 ± 0.5 ns (*skew*) and 1.08 ± 0.1 ns (near-*trans*) in MCH indicates equilibrium between the two emissive species. These results align with PEC simulations indicating that excitation to S_2 is followed by internal conversion to S_1, where the system partitions between the two conformers. These findings were further supported by TRES and TRANES analyses, introduced by Periasamy and co-workers [62–64], which helps to distinguish whether the emission arises from a single species undergoing solvation or from multiple species. The TRANES analyses of 2,2′-pyridil for both fluorescence and phosphorescence bands (Figure 6G,H), indicate a single isoemissive point in each case: 391 nm for fluorescence and 474 nm for phosphorescence, conclusively ruling out higher excited-state fluorescence and confirming that the observed dual fluorescence and dual phosphorescence arise from the two conformations (*skew* and near-*trans*) of the excited molecular system [33].

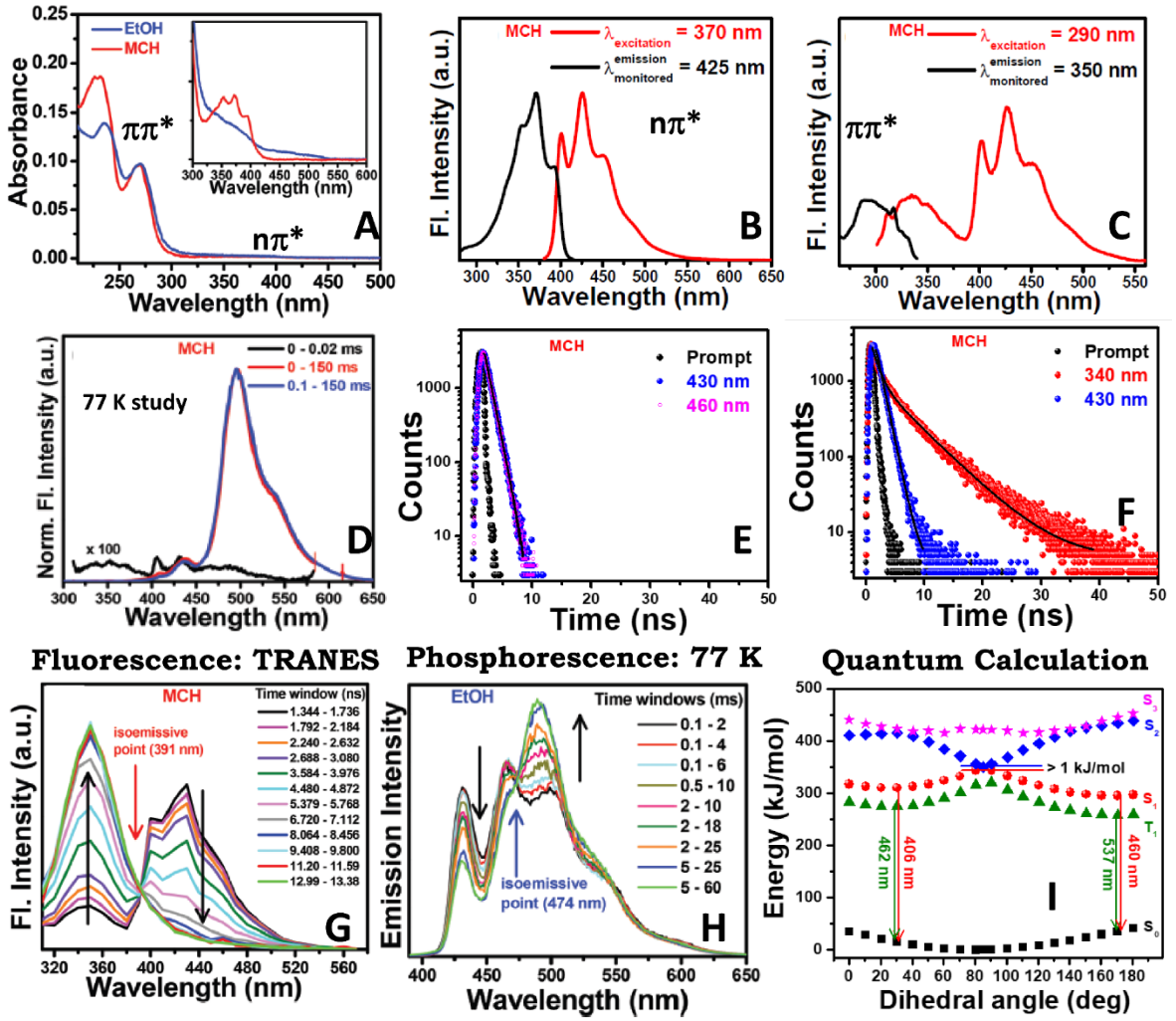

Figure 6. (**A**) Absorption spectrum of 2,2′-pyridil in EtOH and MCH, showing distinct nπ* and ππ* bands. (**B**,**C**) Emission and excitation spectra at room temperature upon (**B**) nπ* and (**C**) ππ* excitations, with excitation and emission wavelengths specified in the legends, showing distinct fluorescence bands. (**D**) Time-resolved emission spectra at 77 K in MCH matrix (λ_{exc} = 290 nm) at varying time windows, distinguishing fluorescence and phosphorescence components. (**E**,**F**) Fluorescence decay profiles upon (**E**) nπ* (λ_{exc} = 370 nm) and (**F**) ππ* (λ_{exc}=

300 nm) excitations. TRANES plots for (**G**) fluorescence at room temperature and (**H**) phosphorescence at 77 K (λ_{exc} = 300 nm), showing isoemissive points that confirm dual conformer equilibria in both S_1 and T_1 states. (**I**) Simulated PECs for the S_0, S_1, S_2, S_3, and T_1 electronic states, illustrating conformational minima, internal conversion pathways, and energetic barriers of 2,2′-pyridil. © 2017 Springer Nature [33].

Low-temperature fluorescence and phosphorescence studies of 2,2′-pyridil in frozen EtOH and MCH matrices at 77 K uncover emissions from distinct excited states and conformers, using aforesaid methodologies established for structurally analogous systems. Time-resolved emission spectra (Figure 6D) clarify the nature of these bands. In the fluorescence timeframe of 0 to 0.02 ms, two weak but clearly distinguishable bands were observed at 310–390 nm and 390–550 nm with peak maxima at 340 nm and 425 nm, respectively. These bands, better resolved in MCH correspond to emissions from near-*trans* and *skew* conformers, which aligns with the observations from room temperature data. Phosphorescence spectra (0.1–150 ms window) reveal two structured bands per matrix. In EtOH, these appear at ~432/465 nm and ~490 nm; in MCH, at ~437 nm and ~496 nm, assigned to T_1 emissions from near-*trans* and *skew* conformers, respectively. These assignments were supported by simulated T_1 potential energy curve (Figure 6I). TRANES analysis in frozen EtOH (Figure 6H) confirms the existence of two triplet species by showing an isoemissive point at 474 nm. With increasing delay time, emission intensity shifts from 410–470 nm (*skew*) to 470–600 nm (near-*trans*), validating the presence of two distinct T_1-state emissive conformers: *skew* and near-*trans*.

Quantum chemical PEC analyses of 2,2′-pyridil across S_0, S_1, S_2, S_3, and T_1 states [Figure 6I] provides potential support in assigning the emissions. Ground-state PEC reveals a single minimum indicating a stable *skew* geometry (Φ = 80.48° in EtOH), consistent with crystallographic data ($\Phi \approx 96.5°$) [53–55]. In contrast, the S_1 PEC exhibits two minima at $\Phi \approx 30°$ and 170°, assigned to the relaxed *skew* and near-*trans* conformers, respectively. The T_1 PEC grossly replicates the S_1 profile, again corroborating involvement of dual triplet conformers in the emission processes. The S_2 state shows a single minimum energy geometry, matching a high-energy S_1 structure, while S_3 exhibits strong solvent stabilization. The minimal energy gap (~1 kJ/mol) between minimum in S_2 and the crest of S_1 facilitates efficient internal conversion, explaining the absence of S_2 emission—unlike in benzil or α-naphthil [22,31]. Barrierless torsion in S_1 enables interconversion between *skew* and near-*trans* forms, accounting for dual fluorescence, with computed emissions at 406 nm (*skew*) and 460 nm (near-*trans*), aligning well with the observed bands (at 400 and 470 nm). Simulated PECs predict phosphorescence at ~462 nm and ~537 nm from the *skew* and near-*trans* forms, respectively, in agreement with experimental results. These DFT/TDDFT findings substantiate the conformer-specific emissions and rationalizes non-observation of the S_2 fluorescence.

Thus, comprehensive photophysical investigations of 2,2′-pyridil at RT and cryogenic conditions establish dual fluorescence and phosphorescence emissions to arise from near-*trans* and relaxed *skew* conformers in both S_1 and T_1 states. The isoemissive point in the TRANES spectra further confirms presence of an equilibrium between the two conformers. Absence of S_2 fluorescence results from an efficient internal conversion from S_2 to S_1, as supported by the simulated potential energy curves, a theoretical support for the experimental findings. Taken together with earlier studies on benzil and α-naphthil, the results on 2,2′-pyridil suggest that S_2 fluorescence is not a general feature of 1,2-dicarbonyl systems, but rather a system-specific phenomenon governed by subtle structural and electronic factors.

5. Searching for S_2 Emission from α-Furil

In the preceding sections, we established that benzil and α-naphthil, both members of the 1,2-dicarbonyl family, exhibit fluorescence from their respective S_2 states, a striking deviation from the traditional photophysics of aromatic systems obeying Kasha's rule of fluorescence [22,31]. However, 2,2′-pyridil, despite its structural resemblance does not show S_2 emission, a phenomenon attributed to its small S_2–S_1 energy gap [33]. These contrasting results prompted us to investigate the issue further with more systems within the family.

To investigate this, we focused on α-furil, a simpler diaromatic 1,2-dicarbonyl compound where two furan rings are connected via a central C–C bond. Owing to reduced steric hindrance from five-membered rings and lesser ortho-proton carbonyl interactions, α-furil offers greater conformational flexibility than benzil [41,65]. Crystallographic studies reveal that α-furil adopts a skew geometry in the ground state with an intercarbonyl (O=C–C=O) dihedral angle of 130.9° [66], whereas theoretical calculations by Lopes et al. predicted a slightly wider angle of ~153° [67]. Photophysical investigations by Singh and Palit demonstrated that the triplet state of α-furil shows negligible conformational deviation from the ground state geometry [68]. Although photoacoustic calorimetric (PAC) investigations indicated a possible *skew*-to-*trans* photoisomerization in α-furil [41], its photoluminescence properties, particularly those originating from higher excited states remained unexplored. With

this prelude, we addressed this gap using strategic steady state and time-resolved spectroscopy, low-temperature (77 K) matrix isolation under controlled illumination [30], and DFT/TDDFT based quantum chemical calculations [32].

Room temperature absorption spectra of α-furil in EtOH and MCH suggests three absorption bands: two higher energy bands at ~225 nm and ~300 nm, and a very weak, broad lowest-energy band at ~420 nm (Figure 7A). Increasing solvent polarity from MCH to EtOH induces negligible bathochromic shifts (~1 nm) for the two higher-energy ππ* bands, but a pronounced hypsochromic shift (~8 nm) for the lowest-energy nπ* band. The minimal solvent-polarity dependence in the absorption spectra of α-furil further indicates a low ground-state dipole moment, consistent with a near trans-planar geometry [32].

Photoexcitation of α-furil at its nπ* absorption band yields a structured fluorescence (390–500 nm) having λ_{max} ~ 430 nm in both EtOH and MCH (Figure 7B). The mirror-image relationship between excitation and emission spectra, along with negligible solvent shifts, indicates this emission from a near trans-planar geometry with a very low dipole moment. Structured emission and concentration-dependent studies rule out the possibility of aggregation, and the band was assigned to S_1 fluorescence of the trans-planar conformer [32,69]. Room temperature excitation at the higher-energy ππ* band (λ_{ex} = 300 nm) drastically modifies the emission pattern of α-furil (Figure 7C). In EtOH, two bands appear at 370 and 434 nm (structured), while in MCH, three emissions were observed with peak maxima at ~ 355 nm, 430 nm (structured), and a weak band at 525 nm. The structured 430 nm band corresponds to the trans-planar S_1 fluorescence, consistent with nπ* excitation. The 525 nm band, present only in MCH, is assigned to phosphorescence from trans-planar triplet conformer (τ~11 μs) [32,41,65,68], absent in EtOH due to triplet quenching by protic solvents [68]. The higher energy 355/370 nm emission, previously unexplored, was attributed to a relaxed skew conformer in the S_1 state, rather than higher-state fluorescence, as supported by its solvent-dependent shift and quantum chemical calculations [32]. Temperature dependent emission studies confirm coexistence of the trans-planar and relaxed skew conformers in the S_1 state, as reflected in the relative variation of their fluorescence intensities.

Room-temperature fluorescence decay profiles of α-furil exhibit mono-exponential decays with lifetimes of 1.40 ± 0.1 ns (EtOH) and 1.11 ± 0.1 ns (MCH) for the 430 nm emission band, corresponding to the trans-planar conformer (Figure 7D). In contrast, excitation at 300 nm revealed bi-exponential decays for the higher-energy emission band (370 nm in EtOH, 355 nm in MCH), with lifetimes of ~1.3 ns and 5–6 ns (Figure 7E). The short component corresponds to the trans-planar conformer, while the longer-lived component was assigned to the relaxed skew conformer in S_1 state, consistent with steady-state spectra and quantum-chemical predictions [32].

At 77 K, upon nπ* excitation (380 nm), both EtOH and MCH glassy matrices display a structured band at 410–490 nm, attributed to S_1 fluorescence from the trans-planar form, along with a weaker 500–650 nm structured band from the triplet state of the same geometry [32]. The phosphorescence intensity is enhanced at 77 K due to suppressed deactivation pathways. Upon ππ* excitation (300 nm), emission spectra depend on freezing conditions. Frozen under dark exhibits only trans-planar fluorescence (410–480 nm) and triplet phosphorescence (500–650 nm). However, frozen in the presence of excitation radiation, results in an additional high-energy fluorescence (~355 nm in MCH, ~370 nm in EtOH), originating from the relaxed skew conformer in S_1 state. Time-window based measurements confirm these assignments: short windows capture both fluorescence bands (355 nm and 430 nm), while long windows reveal two distinct phosphorescence bands: one from the trans-planar conformer (500–650 nm, τ ~ 5 ms) and another higher-energy band (~ 465 nm, τ ~ 80 ms) from the relaxed skew triplet state (Figure 7F,G) [32].

Overall, fluorometric analyses of α-furil in ethanol and MCH, at both room temperature and 77 K, reveal multiple emissions associated with distinct conformers in the singlet and triplet manifolds (Figure 7A–G), supported by quantum chemical calculations. The optimized ground-state structure of α-furil shows an intercarbonyl dihedral angle (O=C–C=O) of 156.1°, with a low dipole moment (μ = 1.73 D), consistent with the experimental observation of insignificant solvent-dependent absorption shifts. Quantum chemical calculations suggest that upon excitation to higher singlet states (S_2 or S_3), α-furil undergoes ultrafast relaxation to S_1 via internal conversion, without exhibiting any detectable S_2 fluorescence. This behavior contrasts with the photophysical characteristics of benzil and α-naphthil, but aligns with that of 2,2′-pyridil [22,31,33]. Non-occurrence of S_2 fluorescence is attributed to proximity (~ 7 kJ/mol) of the minimum of PEC of S_2 electronic state to the potential energy crest of S_1 state. This near-resonance in energy facilitates an ultrafast internal conversion while preserving molecular geometry, enabling relaxation either to the trans-planar minimum (Φ = 180°) or the relaxed skew minimum (Φ ~ 30°). Consequently, two S_1 emissions are expected, consistent with experiment and supported by the simulated potential energy curves (PECs) (Figure 7H) [32]. PEC of the lowest triplet state (T_1) (Figure 7H) further predicts two phosphorescence pathways: ~ 500 nm from the trans-planar form and ~ 451 nm from the relaxed skew form, both in good agreement with experimental observations [32].

Taken together, these findings underscore that S_2 emission is not a universal trait among 1,2-dicarbonyls, but is rather highly system-dependent, modulated by electronic structure, conformational dynamics, and excited-state energetics.

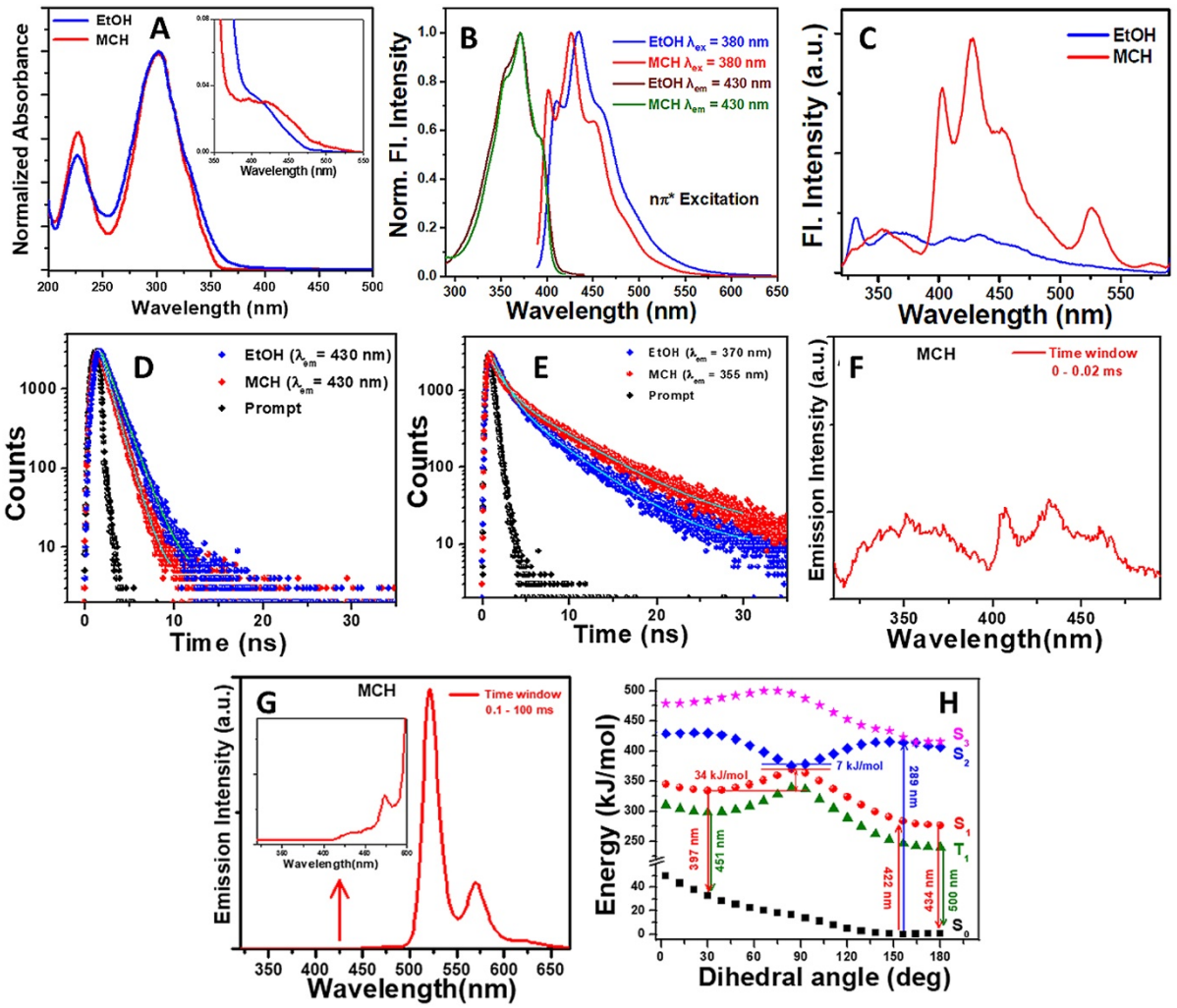

Figure 7. (**A**) Absorption spectrum of α-furil in EtOH and MCH, showing distinct nπ* and ππ* bands. (**B**) Emission and excitation spectra of α-furil at room temperature upon nπ* excitation, with excitation and emission wavelengths specified in the legends and (**C**) Emission spectra upon ππ* excitation (λ_{exc} = 300 nm) in both EtOH and MCH, showing distinct fluorescence bands. Room temperature fluorescence decay profiles monitoring (**D**) trans planer (λ_{exc} = 370 nm) and (**E**) relaxed skew conformers (λ_{exc} = 300 nm) of α-furil in both EtOH and MCH. Emission spectra at 77 K in MCH matrix with varying time windows (λ_{exc} = 300 nm), distinguishing fluorescence (**F**) and phosphorescence (**G**) components. Simulated PECs for the S_0, S_1, S_2, S_3, and T_1 electronic states (**H**), illustrating efficient internal conversion from the S_2 to S_1 state, with no evidence of fluorescence originating from S_2. © 2016 AIP Publishing [32].

6. Photophysics of 9,9′-Anthril: Comparison with Other 1,2-Dicarbonyl Systems

Extensive investigations on the photophysical behavior of benzil, α-naphthil, 2,2′-pyridil and α-furil, all being members of the 1,2-dicarbonyl family, revealed conflicting results in terms of occurrence of S_2 emission. While the former two molecular systems exhibit S_2 emission the latter two don't [22,31–33]. Our comprehensive fluorometric investigations, thus, project that occurrence of S_2 emission is not a general characteristics within this molecular class. To reinforce this conjecture further, photophysical investigations of 9,9′-anthril, a more complicated tricyclic member of the family, was systematically explored through steady state and time resolved experimental observations, supported by DFT and TDDFT based quantum chemical calculations [34].

Absorption studies of anthril in EtOH and MCH solvents reveal two well-resolved absorption bands: a weaker, structured and polarity sensitive nπ* band in 300–450 nm range, and a more intense ππ* band in 220–300 nm region, with marginal solvent dependence (Figure 8A). Blue shift of the lower energy band and nominal red shift of the higher energy band with increasing solvent polarity corroborate nature of their respective electronic transitions as nπ* and ππ* respectively. Studies by Becker et al. along with our quantum chemical calculations,

strongly support a significantly twisted geometry of anthril in its ground state [34,69]. It is interesting to note that for 1,2-dicarbonyl systems, the nπ* absorption maxima correlate well with the intercarbonyl dihedral angle (Φ); greater planarity (Φ approaching 180°) leads to increased conjugation and red-shift of the nπ* band due to decrease in dipole moment and greater stabilization by the solvent [34]. Quantum chemical calculations provide the following Φ values for the studied structurally related systems: benzil (126.6°), α-naphthil (113°), α-furil (156.1°), 2,2′-pyridil (80.5°), and 9,9′-anthril (81.0°) [22,31–34] and a linear relationship is observed between Φ and nπ* band maxima in MCH, a novel observation for 1,2-dicarbonyl family (Figure 8B).

At room temperature upon photoexcitation at its ππ* absorption band (290 nm) in both ethanol and MCH, anthril exhibits dual fluorescence with structured bands. One of these bands (390–570 nm) corresponds to S_1 fluorescence from the near-*trans* conformer (dihedral angle ~169°). This emission is also observed upon excitation at the lower-energy nπ* band (380 nm) (Figure 8C,D). The higher-energy emission band (320–390 nm) was ascribed to originate from a relaxed *skew* conformer in the same S_1 state; rather than from a higher excited state (S_2 or S_3), as supported by DFT/TDDFT-based simulations of the PECs across various electronic states. These two coexisting conformers exhibit distinct dipole moments (0.98 D and 6.1 D), with the relaxed *skew* species showing higher sensitivity towards solvent polarity and contributing more prominently in polar ethanol. The mirror-image relationship between the excitation and emission spectra confirms the emission to be monomeric only.

Time-resolved fluorescence analysis of anthril reveals that excitation at the $n\pi^*$ band yields a single lifetime component (~11 ns), indicative of emission solely from the near-*trans* conformer. However, upon ππ* excitation, bi-exponential fluorescence decay profiles were observed in both ethanol and MCH, corresponding to two lifetimes (~6–7 ns and ~10–11 ns) (Figure 8E), which were assigned to the relaxed *skew* and near-*trans* conformers, respectively. Through exhibiting distinct isoemissive points (400 nm in EtOH and 389 nm in MCH), TRES and TRANES studies (Figure 8F) unambiguously establish the coexistence of two emitting conformers in the S_1 state [34]. These findings, corroborated by simulated PECs, firmly rule out the involvement of higher singlet excited states (S_2 or S_3) and attribute the dual fluorescence solely to structural relaxation into two torsional isomers in the S_1 state. This conformer-specific emission behavior highlights the critical role of excited-state torsional dynamics in modulating fluorescence characteristics in 9,9′-anthril.

The cryogenic emission studies of anthril in EtOH and MCH glassy matrices successfully separated overlapping emissions by temporally resolving fluorescence and phosphorescence bands through time-gated spectroscopy (Figure 8G). Upon excitation at either of the n→π* (380 nm) or π→π* (290 nm) absorption bands, structured fluorescence emissions were observed from two distinct conformers in the S_1-state: a near-*trans* conformer emitting in 400–550 nm range, and a relaxed *skew* conformer emitting at a rather higher energy (310–380 nm). At longer time windows (0.1–100 ms), two well-resolved phosphorescence bands spanning 400–600 nm emerged, with distinct spectral regions and lifetime values. Phosphorescence lifetime analysis revealed that the lower energy band (470–600 nm, ~3 ms) originates from the *trans* conformer in the T_1 state, while the higher energy band (400–470 nm) exhibits exceptionally long lifetimes (~5000 ms), attributed to the *cis* triplet species. Presence of an isoemissive point in the TRANES spectra (at 478 nm) and the agreement with quantum chemical calculations firmly establish the existence of two coexisting triplet conformers (Figure 8H). These findings reveal the intricate role of conformational dynamics in shaping the emissive landscape of 1,2-dicarbonyl systems, and underscore the effectiveness of low-temperature, time-resolved emission spectroscopy as a powerful tool for probing and resolving excited state heterogeneity and photophysical complexity.

Quantum chemical calculations provided compelling theoretical validation for the experimental emission behavior of anthril, revealing a *skew* ground-state geometry, with a torsional angle (Φ) of approximately 81°, and supporting the existence of two distinct conformers—near-*trans* and relaxed *skew* in the S_1 state, each responsible for one of the observed dual fluorescence bands [34]. PECs constructed across S_1, S_2, and S_3 electronic states (Figure 8I) reveal energy proximity across the entire range of Φ values. This points to a facile internal conversion from the higher excited states (S_2 and S_3) to S_1, consistent with the absence of S_2 emission, similar to α-furil [32] and 2,2′-pyridil [33] and contrary to benzil [22] and α-naphthil [31]. Furthermore, T_1 state optimizations confirm two distinct triplet conformers (*trans* and *cis*) corresponding to dual phosphorescence emissions. The isoemissive point observed in the TRANES plot upholds the conformational equilibria in both singlet and triplet manifolds. The computational insights emphasize the critical role of intercarbonyl torsion in dictating the amusing photophysical landscape of anthril.

Comprehensive photophysical investigations, complemented by quantum chemical calculations, thus, reveal that the multiple emissions of 9,9′-anthril originate from distinct conformers in both singlet (S_1) and triplet (T_1) excited states; specifically, relaxed *skew* and near-*trans* in S_1, and *cis* and *trans* in T_1 at room temperature and cryogenic conditions in EtOH and MCH glassy matrices. Dual fluorescence and phosphorescence bands, along with signatures of the presence of equilibrium reflected in the TRES and TRANES spectra, confirm conformational

interconversion within both the aforesaid excited states. Absence of S_2 emission was rationalized from the energetic proximity of the higher singlet states, positioning anthril's behavior closer to α-furil and 2,2′-pyridil, and distinct from S_2-emissive analogues like benzil and α-naphthil. These findings highlight that S_2 fluorescence is not an intrinsic feature of the 1,2-dicarbonyl molecular systems but is governed by molecular specificity within the series.

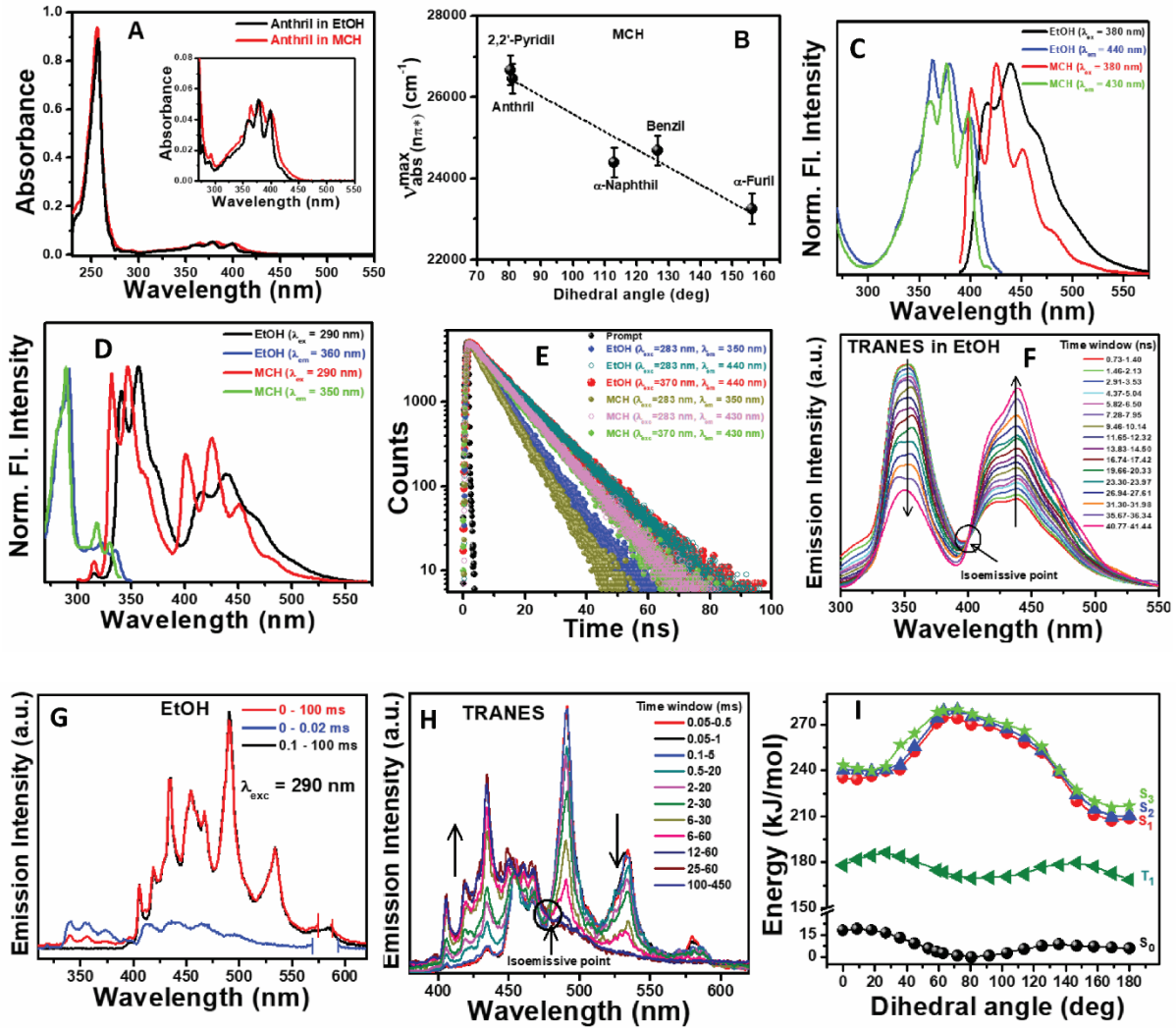

Figure 8. (**A**) UV-Vis absorption spectra of 9,9′-anthril recorded in EtOH and MCH. (**B**) Correlation between the nπ* absorption maxima versus intercarbonyl dihedral angles (Φ) across a set of 1,2-dicarbonyl derivatives, highlighting *skew* geometry of anthril. (**C**,**D**) Emission and corresponding excitation spectra of anthril at room temperature upon (**C**) nπ* (λ_{exc} = 283 nm) and (**D**) ππ* (λ_{exc} = 370 nm) excitations with excitation and emission wavelengths specified in the legends, showing distinct fluorescence bands. (**E**) TCSPC decay profiles upon nπ* and ππ* excitations. (**F**) TRANES analysis at RT (λ_{exc} = 283 nm) evidencing equilibrium between S_1-state conformers. (**G**) Time-resolved emission spectra at 77 K in EtOH at different time windows upon ππ* excitation (λ_{exc}= 290 nm). (**H**) TRANES analysis in EtOH matrix at 77 K (λ_{exc} = 290 nm), confirming the presence of two triplet emissive species. (**I**) Simulated PECs for the S_0, S_1, S_2, S_3, and T_1 electronic states of 9,9′-anthril, illustrating absence of S_2 fluorescence. © 2018 ACS publication [34].

7. Conclusions

The account provides the first in-depth photophysical analysis of a series of multi-emissive molecular systems within the 1,2-dicarbonyl family, namely benzil, α-naphthil, 2,2′-pyridil, α-furil, and 9,9′-anthril, through an integrated approach combining steady-state and time-resolved emission analyses with advanced quantum chemical simulations. A novel experimental approach involving freezing at 77 K under illuminated and dark conditions, alongside TRES and TRANES have been successfully introduced to probe conformer-specific fluorescence and phosphorescence emissions. This review confirms that S_2 emission, a deviation from Kasha's rule, is unambiguously observed for benzil and α-naphthil, but is absent in α-furil, 2,2′-pyridil, and 9,9′-anthril.

This establishes that S_2 emission is not a general characteristic for the members of the 1,2-dicarbonyl family, rather the photophysical behavior is very much system specific governed by the unique electronic and conformational landscapes of the individual molecule. Each system has some characteristic signature on its photophysics as evident from the PECs in different electronic states of the corresponding molecule. These insights set a new benchmark for future photophysical studies and open up new avenues in the exploration of complex excited-state behavior of versatile classes of molecular systems exploiting ultrafast spectroscopy, triplet state dynamics, time-resolved studies at RT as well as cryogenic temperatures, TRES and TRANES, and quantum chemical simulations of PECs/PESs.

Author Contributions

P.K.: Writing—Original Draft, Writing—Review & Editing, Software, Data Curation, Formal analysis, Investigation, Visualization, Methodology; K.N.V.: Assisting in writing, Software; N.C.: Conceptualization, Funding Acquisition, Resources, Supervision, Visualization, Validation, Writing—Review & Editing. All authors have read and agreed to the published version of the manuscript.

Funding

P.K. sincerely thanks Presidency University, Bengaluru, for institutional support. P.K. also acknowledges financial support from DST-SERB, Govt. of India, through project PDF/2020/002667 (NPDF), and N.C. gratefully acknowledges funding from CSIR, Govt. of India, through project 01(3065)/21/EMR-II. K.N.V. thanks Presidency University, Bengaluru, for the University Fellowship.

Institutional Review Board Statement

Not applicable.

Informed Consent Statement

Not applicable.

Data Availability Statement

The data supporting this Account are from our previously published work with copyright permissions obtained; no new data sets were generated.

Conflicts of Interest

The authors declare no conflict of Interest.

References

1. Lakowicz, J.R. *Principles of Fluorescence Spectroscopy*, 3rd ed.; Springer: New York, NY, USA, 2006.
2. Rohatgi-Mukherjee, K.K. *Fundamentals of Photochemistry*; Wiley Eastern: New Delhi, India, 1992.
3. Mataga, N. Photochemical Charge Transfer Phenomena–Picosecond Laser Photolysis Studies. *Pure Appl. Chem.* **1984**, *56*, 1255.
4. Kundu, P.; Banerjee, D.; Maiti, G.; et al. Dehydrogenation Induced Inhibition of Intramolecular Charge Transfer in Substituted Pyrazoline Analogue. *Phys. Chem. Chem. Phys.* **2017**, *19*, 11937.
5. Kundu, P.; Ghosh, S.; Karmakar, R.; et al. Impact of Structural Modification on the Photophysical Response of Benzoquinoline Fluorophores. *J. Fluoresc.* **2016**, *26*, 845.
6. Chattopadhyay, N.; Chowdhury, M. Equilibrium pK* of Carbazole Studied by the Deprotonation Reaction in Ammoniacal Aqueous Media. *J. Photochem.* **1987**, *38*, 301.
7. Mishra, A.K.; Dogra, S.K. Prototropic Equilibria in Lowest Excited Singlet State of 2-Hydroxybenzimidazole 2-(3H) benzimidazolone. *J. Photochem.* **1985**, *29*, 435.
8. Formosinho, S.J.; Arnaut, L.G. Excited-state Proton Transfer Reactions II. Intramolecular Reactions. *J. Photochem. Photobiol. A* **1993**, *75*, 21.
9. Sengupta, P.K.; Kasha, M. Excited State Proton-transfer Spectroscopy of 3-Hydroxyflavone and Quercetin. *Chem. Phys. Lett.* **1979**, *68*, 382.
10. Lewis, G.N.; Magel, T.T.; Lipkin, D. The Absorption and Re-emission of Light by cis- and trans-Stilbenes and the Efficiency of their Photochemical Isomerization. *J. Am. Chem. Soc.* **1940**, *62*, 2973.
11. Mallick, A.; Purkayastha, P.; Chattopadhyay, N. Photoprocesses of Excited Molecules in Confined Liquid Environments: An Overview. *J. Photochem. Photobiol. C Photochem. Rev.* **2007**, *8*, 109–127.

12. Chowdhury, N.K.; El-Sayed, M.A. Molecular Origin of the Optical Rotatory Dispersion of the Benzil Crystal. *J. Chem. Phys.* **1967**, *47*, 1133.
13. Rubin, M.B. In *Photochemistry and Organic Synthesis*; Springer: Berlin/Heidelberg, Germany, 1985; Volume 129.
14. Bera, S.C.; Mukherjee, R.; Chowdhury, M. Spectra of Benzil. *J. Chem. Phys.* **1969**, *51*, 754.
15. Brown, C.J.; Sadanaga, R. The Crystal Structure of Benzil. *Acta Crystallogr.* **1965**, *18*, 158.
16. Cumper, C.W.N.; Thurston, A.P. Electric Dipole Moments and Molecular Conformations of Benzophenones, Benzils, Benzhydrols, and Benzoins. *J. Chem. Soc. Perkin Trans.* **1972**, *2*, 106.
17. Morantz, D.J.; Wright, A.J.C. Structures of the Excited States of Benzil and Related Dicarbonyl Molecules. *J. Chem. Phys.* **1971**, *54*, 692.
18. Evans, T.R.; Leermakers, P.A. Emission Spectra and Excited-state Geometry of Alpha-diketones. *J. Am. Chem. Soc.* **1967**, *89*, 4380.
19. Das, G.; Mohapatra, K.; Bhattacharya, J.; et al. Flash Photolysis of Benzils. *J. Photochem. Photobiol. A* **1987**, *40*, 47.
20. Bertoti, A.R.; Netto-Ferreira, J.C. Absolute Rate Constants for the Reaction of Benzil and 2,2′-Furil Triplet with Substituted Phenols in the Ionic Liquid 1-Butyl-3-methylimidazolium Hexafluorophosphate: A Nanosecond Laser Flash Photolysis Study. *Appl. Chem.* **2024**, *4*, 224–235.
21. Santosh, C.; Mishra, P.C. Electronic Spectra of Benzil in Solution and Thin Film. *J. Photochem. Photobiol. A* **1990**, *51*, 245.
22. Bhattacharya, B.; Jana, B.; Bose, D.; et al. Multiple Emissions of Benzil at Room Temperature and 77 K and Their Assignments from Ab-initio Quantum Chemical Calculations. *J. Chem. Phys.* **2011**, *134*, 044535.
23. Kasha, M. Characterization of Electronic Transitions in Complex Molecules. *Discuss. Faraday Soc.* **1950**, *9*, 14.
24. Beer, M.; Longuet-Higgins, H.C. Anomalous Light Emission of Azulene. *J. Chem. Phys.* **1955**, *23*, 1390.
25. Bajema, L.; Gouterman, M.; Rose, C.B. Porphyrins XXIII: Fluorescence of the Second Excited Singlet and Quasiline Structure of Zinc Tetrabenzporphin. *J. Mol. Spectrosc.* **1971**, *39*, 421.
26. Hui, M.H.; de Mayo, P.; Suau, R.; et al. Thione Photochemistry: Fluorescence from Higher Excited States. *Chem. Phys. Lett.* **1975**, *31*, 257.
27. Chattopadhyay, N.; Barroso, M.; Serpa, C.; et al. Photophysics of 3-hydroxyflavone in supercritical CO_2: A probe to study the microheterogeneity of the environment. *Chem. Phys. Lett.* **2004,** *387*, 263.
28. Cho, D.W.; Fujitsuka, M.; Ryu, J.H.; et al. S_2 Emission from Chemically Modified BODIPYs. *Chem. Commun.* **2012**, *48*, 3424.
29. Zhang, X.; Loh, K.P.; Sullivan, M.B.; et al. Aggregation Dependent S_1 and S_2 Dual Emissions of Thiophene−Acrylonitrile−Carbazole Oligomer. *Cryst. Growth Des.* **2008**, *8*, 2543.
30. Chattopadhyay, N.; Serpa, C.; Arnaut, L.G.; et al. Coexistence of two Triplets for the TICT Probe DMABN in Polar Solvents: An Experimental Evidence. *Helv. Chim. Acta* **2002**, *85*, 19.
31. Jana, B.; Chattopadhyay, N. Multiple Emissions of α-Naphthil: Fluorescence from S_2 State. *J. Phys. Chem. A* **2012**, *116*, 7836.
32. Kundu, P.; Chattopadhyay, N. Photophysics of α-furil at Room Temperature and 77 K: Spectroscopic and Quantum Chemical Studies. *J. Chem. Phys.* **2016**, *144*, 234317.
33. Kundu, P.; Ghosh, S.; Chattopadhyay, N. Exploration of Photophysics of 2,2′-Pyridil at Room Temperature and 77 K: A Combined Spectroscopic and Quantum Chemical Approach. *Photochem. Photobiol. Sci.* **2017**, *16*, 159.
34. Kundu, P.; Chattopadhyay, N. Photophysics of Anthril in Fluids and Glassy Matrixes. *J. Phys. Chem. A* **2018**, *122*, 5545.
35. Arnett, J.; McGlynn, S.P. Photorotamerism of Aromatic α-Dicarbonyls. *J. Phys. Chem.* **1975**, *79*, 626.
36. Chan, I.Y.; Heath, B.A. An ENDOR Study of the Geometry of the Lowest Triplet State of Benzil. *J. Chem. Phys.* **1979**, *71*, 1070.
37. Roy, D.S.; Bhattacharyya, K.; Bera, S.C.; et al. Conformational Relaxation in the Excited Electronic States of Benzil and Naphthyl. *Chem. Phys. Lett.* **1980**, *69*, 134.
38. Bhattacharyya, K.; Ray, D.S.; Chowdhury, M. Fluorescence from Relaxed and Unrelaxed Excited State of Benzil. *J. Lumin.* **1980**, *22*, 95.
39. Bhattacharyya, K.; Chowdhury, M. Solvent Shift and Excited State Geometries of Benzil. *J. Photochem.* **1986**, *33*, 61.
40. Chakarabarty, A.; Purkayastha, P.; Chattopadhyay, N. Laser Induced Optoacoustic Spectroscopy of Benzil: Evaluation of Structural Volume Change upon Photoisomerization. *J. Photochem. Photobiol. A* **2008**, *198*, 256.
41. Sarkar, D.; Chakrabarty, A.; Chattopadhyay, N. Structural Volume Change upon Photoisomerization of 2,2′-Furil: A Photoacoustic Calorimetric Study. *Indian J. Chem. Sect. A* **2009**, *48*, 45.
42. Singh, A.K.; Palit, D.K.; Mittal, J.P. Conformational Relaxation Dynamics in the Excited Electronic States of Benzil in Solution. *Chem. Phys. Lett.* **2002**, *360*, 443.
43. Chattopadhyay, N.; Serpa, C.; Silva, M.I.; et al. Benzil Fluorescence and Phosphorescence Emissions: A Pertinent Probe for the Kinematic Behaviour and Microheterogeneity of Supercritical CO_2. *Chem. Phys. Lett.* **2001**, *347*, 361.
44. Das, K.K.; Majumdar, D. Ground and Excited States of Benzil: A Theoretical Study. *J. Mol. Struct. Theochem.* **1993**, *288*, 55.
45. Pawelka, Z.; Koll, A.; Zeegers-Huyskens, T. Solvent Effect on the Conformation of Benzil. *J. Mol. Struct.* **2001**, *597*, 57.

46. Tétreault, N.; Muthyala, R.S.; Liu, R.S.H.; et al. Control of the Photophysical Properties of Polyatomic Molecules by Substitution and Solvation: The Second Excited Singlet State of Azulene. *J. Phys. Chem. A* **1999**, *103*, 2524.
47. Strickler, S.J.; Berg, R.A. Relationship Between Absorption Intensity and Fluorescence Lifetime of Molecules. *J. Chem. Phys.* **1962**, *37*, 814.
48. Herkstroeter, W.G.; Lamola, A.A.; Hammond, G.S. Mechanisms of Photochemical Reactions in Solution. XXVIII.1 Values of Triplet Excitation Energies of Selected Sensitizers. *J. Am. Chem. Soc.* **1964**, *86*, 4537.
49. Debnath, R.; Bera, S.C. Emission Spectra of α-naphthil. *J. Phys. Chem.* **1980**, *84*, 2623.
50. Sen, D.; Manna, B.K.; Bera, S.C. Flash Photolysis of α-Naphthil in the Temperature Range 77 to 320 K. *J. Photochem. Photobiol. A* **1991**, *60*, 101.
51. Sen, D.; Manna, B.K.; Bera, S.C. Spectra and Conformation of α-Naphthil. *J. Mol. Struct.* **1992**, *271*, 45.
52. Shimada, R.; Goodman, L. Polarization of Aromatic Carbonyl Spectra. *J. Chem. Phys.* **1965**, *43*, 2027.
53. Bernal, I. Molecular Configuration of Benzil and α-Pyridil. *Nature* **1963**, *200*, 1318.
54. Ashida, T. The Crystal Structure of 2,2′-Pyridil, a Refinement. *Acta Crystallogr. Sect. B: Struct. Crystallogr. Cryst. Chem.* **1970**, *26*, 454.
55. Barassin, J. Sur La Configuration Moleculaire De Quelques Derives De La Pyridine Et Du Phenyl-N Succinimide. 1. Introduction. *Ann. Chim.* **1963**, *8*, 637.
56. Migchels, P.; Maes, G.; Zeegers-Huyskens, T.; et al. Infrared and Ultraviolet Investigation of the Conformation and Proton Acceptor Ability of 2,2′-Pyridil. *J. Mol. Struct.* **1989**, *193*, 223.
57. Inone, H.; Nagaya, K. Hydrogen Bonding and Conformational Change of 2,2′-Pyridil in Polyhydric Solvents. *J. Chem. Soc. Perkin Trans. 2* **1983**, *2*, 1581.
58. Sarkar, A.; Chakravorti, S. Photo-rotamerism of 2,2′-Pyridil in Different Environments: A Guest for Geometry in Excited States. *J. Lumin.* **1996**, *69*, 161.
59. Sarkar, S.K.; Ghoshal, S.K.; Kastha, G.S. Effect of Ring aza Substitution on the Luminescence of Aromatic Ketones. Luminescence of Isomeric Acetylpyridines. *Proc. Indian Acad. Sci. Chem. Sci.* **1983**, *92*, 47.
60. Bera, S.C.; Mukherjee, R.K.; Mukherjee, D.; et al. n→π* Transition of 2, 2′-Pyridil. *J. Chem. Phys.* **1971**, *55*, 5826.
61. Warwick, D.A.; Wells, C.H. Perturbation of Singlet—Triplet Transitions in Aromatic Carbonyl Compounds. *Spectrochim. Acta* **1968**, *24*, 589.
62. Koti, A.S.R.; Periasamy, N. Application of Time Resolved Area Normalized Emission Spectroscopy to Multicomponent Systems. *J. Chem. Phys.* **2001**, *115*, 7094.
63. Koti, A.S.R.; Krishna, M.M.G.; Periasamy, N. Time-resolved Area-normalized Emission Spectroscopy (TRANES): A Novel Method for Confirming Emission from two Excited States. *J. Phys. Chem. A* **2001**, *105*, 1767.
64. Koti, A.S.R.; Periasamy, N. Time Resolved Area Normalized Emission Spectroscopy (TRANES) of DMABN Confirms Emission from two States. *Res. Chem. Intermed.* **2002**, *28*, 831.
65. Sandroff, C.J.; Chan, I.Y. Triplet Emission from Furil in Different Crystalline Environments: Optical and ODMR Studies. *Chem. Phys. Lett.* **1983**, *97*, 60.
66. Biswas, S.C.; Ray, S.; Podder, A. Molecular Configuration of α-Furil. *Chem. Phys. Lett.* **1987**, *134*, 541.
67. Lopes, S.; Gómez-Zavaglia, A.; Fausto, R. Matrix Isolation and low Temperature Solid State FTIR Spectroscopic Study of α-Furil. *Phys. Chem. Chem. Phys.* **2006**, *8*, 1794.
68. Singh, A.K.; Palit, D.K. Excited-state Dynamics and Photophysics of 2, 2′-Furil. *Chem. Phys. Lett.* **2002**, *357*, 173.
69. Becker, H.D.; Sorensen, H.; Hammarberg, E. 9,9′-Anthril (di-9-anthrylethanedione). *Tetrahedron Lett.* **1989**, *30*, 989.